

## Comparison of the Bhatnagar-Gross-Krook approximation with the exact Coulomb collision operator

S. Livi and E. Marsch

*Max-Planck-Institut für Aeronomie, Postfach 20, D-3411 Katlenburg-Lindau, Federal Republic of Germany*

(Received 22 November 1985)

The collisional relaxation of a bi-Maxwellian and a double-beam distribution is studied in order to assess the reliability of the Bhatnagar-Gross-Krook (BGK) operator in comparison with the full Fokker-Planck Coulomb collision operator. If a velocity-dependent relaxation rate is employed, qualitative agreement can be achieved between both models. Using the friction rate  $\nu_F$  in the BGK model yields numerical results most similar to those of the exact Fokker-Planck model. However, in quantitative terms the collisional relaxation of higher moments is only poorly described. In particular, for the skewness or heat flux the numerical differences are intolerable. For this and other reasons detailed in the paper, the BGK model cannot serve as a reliable calculation of transport properties. Nevertheless, it may have merits in qualitatively assessing collisional effects in inhomogeneous systems which otherwise have to be treated as entirely collision-free.

### I. INTRODUCTION

The aim of this paper is to analyze numerically the collisional relaxation in time of a bi-Maxwellian and a double-beam distribution function by employing the Bhatnagar-Gross-Krook (BGK) collision operator<sup>1</sup> for various velocity-dependent collision rates and to compare the results with the exact evolution obtained by time integration of the Fokker-Planck collision operator.<sup>2</sup> By this procedure a detailed comparison is facilitated between the shape and the moments of the instantaneous distribution function. The relaxation-time approximation can thus be assessed not only qualitatively but also quantitatively, which helps to judge its reliability for various applications in plasma physics.

Generally speaking, the BGK collision term turns out to be a poor approximation for the collisional relaxation of all velocity moments higher than the mean temperature. In particular, the heat-flux regulation is rather inappropriately described.

An explicit solution of the Boltzmann equation<sup>3</sup> or the Fokker-Planck equation<sup>4</sup> is generally a matter of considerable difficulty and in most realistic physical systems practically impossible. With the advent of modern computers, however, numerical solutions<sup>5</sup> have become available, accounting even for complicated boundary and initial conditions and time-varying forces in gases and multispecies plasmas.<sup>6</sup> Still, for many applications approximate analytical solutions are required, which allow better insight into the problem at hand and contribute to physical intuition. In the collision-dominated regime, the machinery of the Chapman-Enskog<sup>3</sup> theory and Grad's method<sup>7</sup> yield approximations to any desired degree by expansion of the distribution function about a Maxwellian to increasing order in the smallness parameter  $l_c/L$ , i.e., free mean path over the macroscale.<sup>8-10</sup> Classical transport theory is based on this approach.

The opposite extreme case is the weakly collisional re-

gime with  $l_c/L \geq 1$ , which is realized in most dilute gases, planetary exospheres,<sup>11</sup> tenuous space plasmas,<sup>12</sup> and laboratory plasmas covering a wide range of density and temperatures. These systems are often treated by disregarding collisions entirely so as to exploit Liouville's theorem for tracing the dynamical evolution of the distribution function.<sup>13,14</sup> The subsequent introduction of collisions then proves to be extremely difficult and no general techniques exist to treat the Boltzmann equation in this case. Since it is desirable to have a single collision operator which covers the whole parameter range of  $0 < l_c/L < \infty$ , Krook and co-workers<sup>1,15</sup> originated what has become known as the BGK model. This is a relaxation-time approach to the collision operator reading

$$\left. \frac{\partial f}{\partial t} \right|_c = -\frac{1}{\tau}(f - f_M), \quad (1)$$

where  $f_M$  is the equivalent Maxwellian with the same value of the density  $n$ , temperature  $T$ , and velocity  $\mathbf{u}$ , as obtained from the original distribution by taking appropriate moments in velocity space.

With a constant  $\tau$  the collision operator (1) is strictly consistent with particle number, momentum, and energy conservation. This statement can be considered as the shortest "derivation" of the BGK model, since the conservation property is indispensable and  $\tau$  is only a phenomenological parameter. Its choice may be justified by plausibility arguments, as given, e.g., by Liboff<sup>16</sup> in relation to the full Boltzmann collision integral. However,  $\tau$  does not follow in any logical manner from first principles. At best, it is a free parameter or function of velocity, which has to be chosen such that the full Boltzmann collision integral is most closely simulated.

If  $\tau(\mathbf{v})$  is a velocity-dependent relaxation time, the problem arises that (1) violates the conservation laws. Particle density, momentum, and energy are then artificially created by "collisions" at each instant of time. One

of the main purposes of this paper is to assess the numerical degree of this violation by using various relaxation rates, e.g., as established by Spitzer<sup>17</sup> for Coulomb collisions. It will turn out that even for strongly velocity-dependent collision rates the density, velocity, and temperature are still conserved within a few percent. In this respect, the usefulness of the BGK collision operator is emphasized by our analysis.

This model derives its importance from its simplicity and the possibility, e.g., to study damping of sound waves in gases and of collective oscillations in plasma in an algebraically tractable way. The original intent of Bhatnagar, Gross, and Krook<sup>1</sup> was to examine the dynamic properties of gases over a continuous range of pressures from the Knudsen to the high-pressure aerodynamic limit. It was then extended to study damping of small-amplitude waves in two-component plasmas.<sup>15</sup> By utilizing a Krook-type collision integral, studies have also been carried out to analyze electrostatic waves in inhomogeneous plasmas in the laboratory,<sup>18,19</sup> and to investigate a plasma instability resulting in field-aligned irregularities in the Earth's ionosphere.<sup>20</sup> Kinetic models with relaxation-time operators have also been developed for gas mixtures<sup>21</sup> by employing the known time scales for energy and momentum exchange between nonequipartition gases with various collisional cross sections.<sup>22</sup>

Since the operator (1) does not involve velocity derivatives, it is easy to work with and, to give an example, one may simply solve kinetic equations by time integration along ballistic collisionless orbits. This technique has been used to study collisional effects on fluid instabilities in an inhomogeneous confined fusion plasma,<sup>18,19</sup> and more recently in the solar-wind context, to model the collisional effects on electrons,<sup>23,24</sup> particularly the so-called "strahl" electrons.<sup>25</sup>

## II. BASIC EQUATIONS AND RELAXATION RATES

As mentioned above, the Krook operator derives its usefulness mainly from its simple algebraic structure and the relaxation-time concept. This has to be contrasted with the full Fokker-Planck operator<sup>2,4,10</sup> which for Coulomb self-collisions can formally be written in a relaxation-time form as well, reading

$$\left. \frac{\partial f}{\partial t} \right|_c = \frac{1}{\tau_0} \nu f \quad (2)$$

with an effective relaxation rate<sup>26,27</sup>

$$\nu(\mathbf{v}) = 2\pi \hat{f}(\mathbf{y}) + \frac{1}{4} \left[ \frac{\partial^2}{\partial \mathbf{y} \partial \mathbf{y}} g(\mathbf{y}) \right] : \left[ \frac{1}{\hat{f}} \frac{\partial^2 \hat{f}}{\partial \mathbf{y} \partial \mathbf{y}} \right] \quad (3)$$

whereby velocities have been normalized as  $\mathbf{y} = \mathbf{v}/v_0$ . For  $v_0$  we may conveniently choose the thermal speed of the equivalent Maxwellian  $f_M$  having the same temperature, mean velocity, and density as  $f$  itself. The distribution  $\hat{f}$  is dimensionless (normalized to a density of 1) and  $g(\mathbf{y})$  is the Rosenbluth potential.<sup>2</sup>

The basic Coulomb collision time is<sup>2,10</sup>

$$1/\tau_0 = \frac{8\pi e^4 n \ln \Lambda}{m^2 v_0^3} \quad (4)$$

which is employed as the natural collision time scale throughout the paper. The BGK operator can be cast in a form similar to (2) by rewriting it as

$$\left. \frac{\partial f}{\partial t} \right|_c = \frac{1}{\tau_0} \nu_{\text{BGK}}(\mathbf{v}) f, \quad (5)$$

where the function  $\nu_{\text{BGK}}$  is

$$\nu_{\text{BGK}}(\mathbf{v}) = \nu_c(\mathbf{v}) \left[ \frac{f_M(\mathbf{v})}{f(\mathbf{v})} - 1 \right]. \quad (6)$$

Equations (2) and (5) look formally alike. Note, however, that  $\nu$  is, via the second derivative of  $f$ , much more sensitive to the actual shape of the distribution function. On the other hand  $\nu_{\text{BGK}}$  depends only on the free function  $\nu_c(\mathbf{v})$ , describing the collisional relaxation, and on the ratio of the equivalent Maxwellian to the actual distribution function. The rewritten form of the collision operators considerably eases comparison of these two models. It also allows one to trace the collisional evolution in time of the instantaneous relaxation rates.

As emphasized in the Introduction, the collision rate  $\nu_c(\mathbf{v})$  is a free model function to be chosen appropriately for the system and type of collisions under consideration. Spitzer<sup>17</sup> has provided a classical analysis of test-particle slowing down, deflection, and energy loss suffered by impinging on a Maxwellian target distribution. The corresponding collision rates are defined in terms of the error function  $\phi(y)$  and its derivative. These rate functions are directly related to velocity-space friction and diffusion<sup>2,4,10</sup> (longitudinal and transverse) and given as

$$\nu_F(y) = \frac{\phi(y) - y\phi'(y)}{y^2}, \quad (7)$$

$$\nu_L(y) = \nu_F/y, \quad (8)$$

$$\nu_T(y) = \frac{(2y^2 - 1)\phi + y\phi'}{2y^3}. \quad (9)$$

Spitzer's slowing down rate is equal to  $\nu_L$  and the deflection rate is

$$\nu_D(y) = \nu_T(y)/y^2. \quad (10)$$

The functions (7)–(10) are velocity dependent and rapidly decline to zero according to power laws at large  $y$  indicating runaway or breakdown of collisional friction and diffusion at high test-particle speeds. We shall employ all four rate functions as collision rate  $\nu_c$  in the BGK operator (5) and (6). The basic time scale  $\tau_0$  is the same in all cases. It is only based on the conserved density and temperature. Finally, we also use the two constant rates

$$\nu_{DT} = \nu_D(1) = \frac{\phi(1) + \phi'(1)}{2}, \quad (11)$$

$$\nu_{FL} = \nu_F(1) = \phi(1) - \phi'(1) \quad (12)$$

in order to demonstrate the differences between strong velocity dispersion in the collision rate  $\nu_c$  and a rigid relaxation at constant  $\nu_c$ . All the rates (7)–(10) are plotted

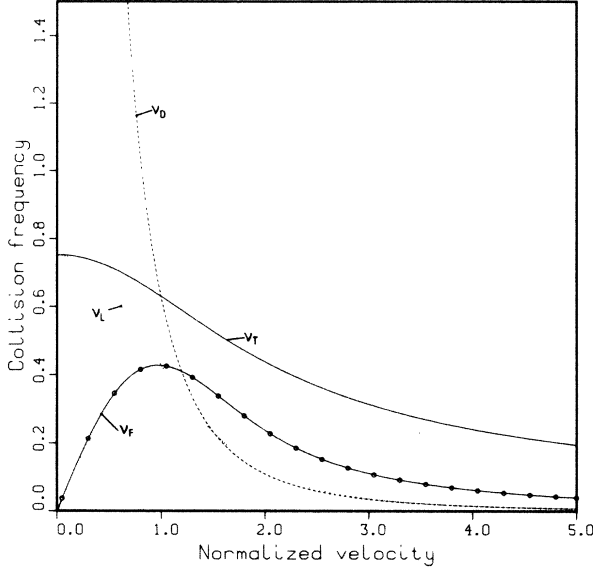


FIG. 1. Collision frequencies as a function of normalized velocity  $y = v/v_0$ .

versus speed in Fig. 1. Note that at  $y=1$  all the rates are about equal, but considerable differences occur at zero and several thermal speeds. The actual course of  $v_c$  as a function of  $y$  has to be kept in mind in order to understand the detailed numerical results presented below. We may finally note that the rate functions for other types of interactions, such as between Maxwell molecules and neutral particles, are also available. They all can be derived from a generalized Rosenbluth potential<sup>28</sup> which reflects the underlying central interaction force and the shape of the target distribution. The rate functions discussed above also play a key role in the transfer by Coulomb collision of energy and momentum between drifting Maxwellians.<sup>10,29,30</sup>

The collision rates  $v_{F,L,T,D}$  are derived from the equivalent Maxwellian with thermal speed  $v_0$  and do not reflect the actual shape of the underlying distribution as does the exact  $v$  of Eq. (3). Rawls *et al.*<sup>31</sup> have proposed modifying the slowing-down rate by rescaling the speed

$v_0$  as  $v_0/\lambda$  which means replacing the true temperature by an effective (parameter  $\lambda$ ) temperature. We considered a similar modification by replacing, for gyrotropic distributions,  $v_0$  by  $v_0(\theta) = (v_{T1}^2 \sin^2 \theta + v_{T\parallel}^2 \cos^2 \theta)^{1/2}$  where  $\theta$  is the pitch angle of the particle velocity with respect to the magnetic field (symmetry axis of the distribution). Then  $y = v/v_0(\theta)$  and consequently  $v_c(y)$  is a true vector function of the velocity. It will be shown later that working with an effective thermal speed related to the particle's pitch angle does not improve the BGK model. These results will not be discussed in detail. Numbers can be read off from Table I. Best agreement with the exact operator was obtained if the rates were isotropic and based on the equivalent Maxwellian  $f_M$ . This is demonstrated in the subsequent section.

### III. NUMERICAL RESULTS

Two nonthermal distributions will be studied here. One is a double-beam distribution with the following parameters  $n=0.8N$  ( $0.2N$ ),  $u = -0.35v_0$  ( $1.4v_0$ ),  $v_T=0.9v_0$  ( $0.6v_0$ ) for the main (beam) component. The effective thermal speed is  $v_0^2 = \sum_j n_j (v_{Tj}^2 + \frac{2}{3} u_j^2)$  with the index running over the two components. These parameters are typical for solar-wind proton distributions.<sup>32,33</sup> We have  $N = n_B + n_M$  and  $u_B n_B + u_M n_M = 0$  (proper frame condition). The distribution function reads

$$f(\mathbf{v}) = \sum_j \frac{n_j}{(\pi v_{Tj})^{3/2}} \times \exp \left[ -\frac{(v_{\parallel} - u_j)^2 + v_{\perp}^2}{v_{Tj}^2} \right]. \quad (13)$$

Secondly, we analyze a bi-Maxwellian distribution with  $v_{T\parallel}^2 = v_0^2/3$  and  $v_{T\perp}^2 = 4v_0^2/3$  yielding  $v_0^2 = (v_{T\parallel}^2 + 2v_{T\perp}^2)/3$  and  $T_{\perp} = 4T_{\parallel}$ .

The collisional decay of these two model distribution towards equilibrium has extensively been analyzed before, in particular the temporal evolution of the effective relaxation rate and the reshaping of  $f$  into a Maxwellian. We refer the reader to the paper of Livi and Marsch<sup>34</sup> which we shall use as our benchmark case which the BGK approximation has to be compared with. Details of the nu-

TABLE I. Results for bi-Maxwellian and double-beam distributions.

	(a) Bi-Maxwellian distribution				(b) Double-beam distribution					
	$N$	$T$	$A$	$\tau_c$	$N$	$u/v_0$	$T$	$A$	$\tau_c$	$\hat{Q}_{\parallel}$
$v_T(\theta)$	-1%	+0.2%	-16%	$2.5 \pm 0.4$	-1%	+0.6%	-1%	-20%	$1.4 \pm 0.3$	-110%
$v_L$	-4%	+0.5%	+33%	$7.8 \pm 1.0$	-2.7%	+2%	-3%	-13%	$3.3 \pm 0.6$	+120%
$v_D(\theta)$	-6%	+3%	+32%	$7.5 \pm 0.9$	-3%	+3%	-3%	-13%	$3.1 \pm 0.7$	+140%
$v_F(\theta)$	-1%	-1%	+13%	$4.6 \pm 0.7$	-3%	+0.5%	-2%	+3.6%	$2.2 \pm 0.4$	-60%
$v_T$	-0.1%	+1%	-17%	$2.3 \pm 0.3$	+0.4%	+1.2%	-0.2%	+20%	$1.5 \pm 0.3$	-85%
$v_L$	-0.5%	+2%	+22%	$5.8 \pm 0.8$	+0.2%	+4%	-1%	-16%	$3.6 \pm 0.7$	+100%
$v_D$	-2%	+3%	+19%	$5.2 \pm 0.9$	+0.3%	+5%	-0.8%	-16%	$3.4 \pm 0.8$	+160%
$v_F$	+0.7%	+1%	+7%	$3.9 \pm 0.5$	+0.1%	+1.5%	-0.5%	+2%	$2.3 \pm 0.4$	-13%
$v_{FL}$	0	0	-11%	$2.7 \pm 0.4$	0	0	0	+15%	$1.6 \pm 0.3$	-120%
$v_{DT}$	0	0	-26%	$1.8 \pm 0.3$	0	0	0	+27%	$1.1 \pm 0.2$	-180%

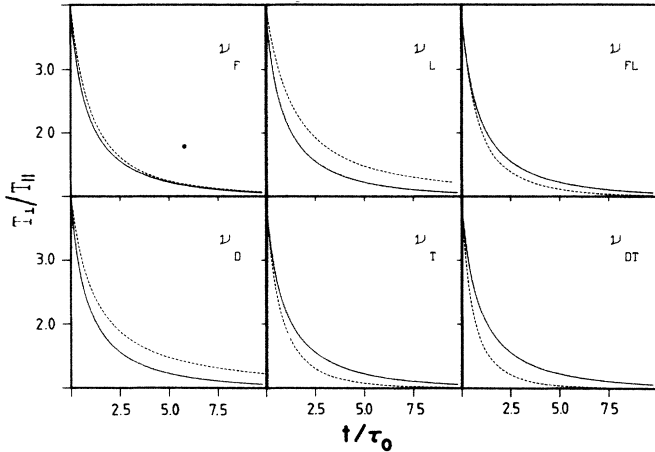


FIG. 2. Temperature ratio  $T_{\perp}/T_{\parallel}$  of an initially bi-Maxwellian distribution function as a function of time in units of  $\tau_0$ . Solid lines relate to the Fokker-Planck, dashed lines display the respective BGK model results with collision rates as indicated. Note the quasiexponential relaxation towards isotropy.

merical treatment of the exact Coulomb collision operator can be found in the above reference and in a more general context in the reviews by Killeen *et al.*<sup>6,35</sup>

Figure 2 shows the collisional relaxation of the bi-Maxwellian distribution towards isotropy. In each box we show the results of the exact and BGK model for  $T_{\perp}/T_{\parallel}$  as a function of time in units of  $\tau_0$  and for the six relaxation rates  $\nu_{F,D,L,T}$ ,  $\nu_{DT}$ , and  $\nu_{FL}$ . We remind the reader of the speed dependence of the rates as displayed in Fig. 1. The temperature anisotropy in Fig. 2 decays almost exponentially for all six cases. Apparently, the rate  $\nu_F$  most closely simulates the true collisional evolution (continuous curves) whereas  $\nu_D$  and  $\nu_L$  retard and  $\nu_T$  accelerates the isotropization process. Note that  $\nu_T \approx 1/y$ ,  $\nu_F \approx 1/y^2$ ,  $\nu_L \approx 1/y^3$ ,  $\nu_D \approx 1/y^3$ , for  $y \gg 1$ . As a result of this asymptotic behavior the rate  $\nu_T$  overestimates and  $\nu_L$  underestimates the true relaxation in the tails of the distribution. In surprising contrast,  $\nu_F$  somehow comes very close to the “truth.” The last two boxes indicate that a constant rate tremendously accelerates the temperature isotropization. The simple reason is that collisional diffusion in the tail at speeds  $y > 1$  is grossly overestimated by fixing the rates at their most probable values at  $y=1$ .

Figure 1 shows that the relaxation rate in the core part of the distribution is smallest for  $\nu_F$ , almost constant for  $\nu_T$  and  $\nu_L$ , and diverges for  $\nu_D$ . Again, small rates about the origin of velocity space seem to be most appropriate in the BGK model to similarly reproduce the results of the full Fokker-Planck operator. These general considerations should be kept in mind in the subsequent discussion.

Table I composes the numerical parameters with relative errors and uncertainties. The upper part of the table relates to the rates evaluated with the pitch-angle-dependent thermal speed  $v_0(\theta)$  and the lower part to rates based on the isotropic  $v_0$  of the equivalent Maxwellian. In each panel the relative maximum error is given. The results with a constant  $v_0$  are generally better than those

with a pitch-angle-dependent relaxation rate as can be inferred by comparison with Table I(a). The column labeled with  $\tau_c$  gives the average  $e$ -folding time for the quasi-exponential decay of  $A = T_{\perp}/T_{\parallel}$  toward 1 in Table I(b). The exact result is  $\tau_c = (3.4 \pm 0.3)\tau_0$ . As can be seen,  $\nu_F$  guarantees density and temperature conservation within a percent and ensures that the actual temperature ratio deviates by no more than 7% from the true value. Whereas density and average temperature are conserved equally well by all rates employed, the collision rate  $\nu_F$  yields best results as far as the anisotropy is concerned.

In Fig. 3 the collisional relaxation of  $T_{\parallel}/T_{\perp}$  for the double-beam distribution (13) is shown. Overall trends are similar to those in Fig. 2. Apparently, the constant rates  $\nu_{DT}$  and  $\nu_{FL}$  accelerate the isotropization process in an unrealistic fashion. Again  $\nu_F$  turns out to be the best choice for the relaxation rate. The corresponding curve (in the upper left box) almost exactly traces the “true” result obtained from the numerical solution of the Fokker-Planck equation. In conclusion, the temperature anisotropy relaxation is fairly well described by the simple BGK model with  $\nu_F$ , even in case of as large an initial ratio as  $T_{\perp}/T_{\parallel} = 4$  in the bi-Maxwellian case. If we consider the next higher moment, i.e., the heat flux related to skewness in the distribution, the situation becomes worse.

In Fig. 4 the collisional reduction of the heat flux, associated with the double-beam distribution, is shown versus time in units of  $\tau_0$ . Apparently, there is stronger dispersion between the true and the BGK model results. The agreement is again best for  $\nu_F$ , although differences between the dashed and the continuous lines are substantial. The collisional decay of the beam is slowest for  $\nu_{D,L}$ . The main reason is that, according to Fig. 1, the rate functions rapidly go to zero beyond  $y=1$ . In contrast  $\nu_F$  has its maximum near this point and runaway sets in only at larger speeds. Consequently, with  $\nu_{D,L}$  employed frictional slowing down is dramatically underestimated and even after about  $10\tau_0$  the beam remains resolved and almost unchanged. In contrast, the rate  $\nu_T$  leads to a much too rapid slowing down of the beam and disappearance of the

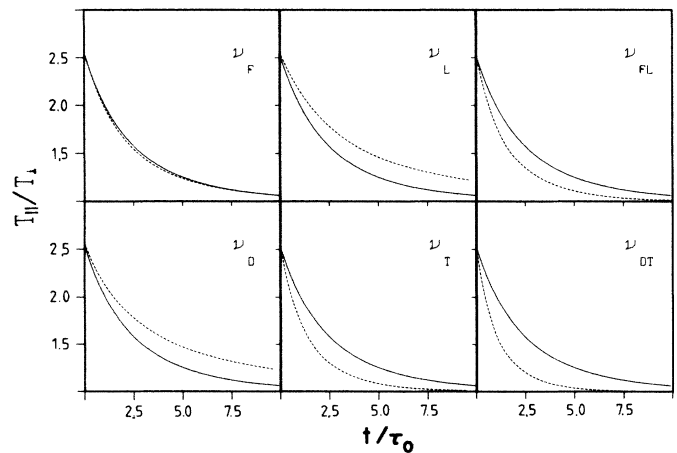


FIG. 3. Temperature ratio  $T_{\parallel}/T_{\perp}$  of an initially resolved double-beam distribution as a function of time in units of  $\tau_0$  in the same format as in Fig. 2.

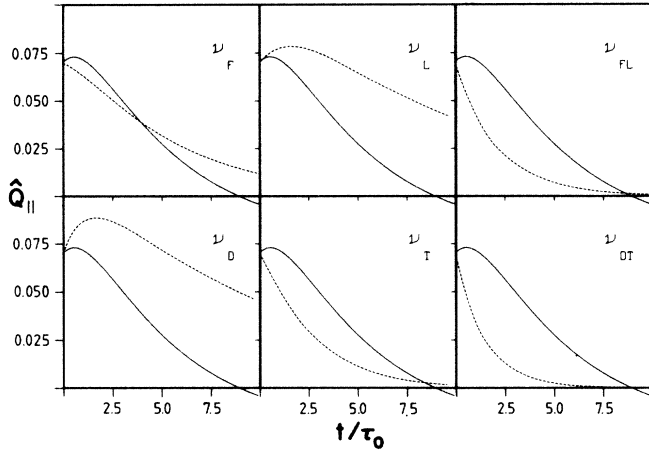


FIG. 4. Normalized heat flux  $\hat{Q}_{||}$  as a function of time in units of  $\tau_0$ . Results for various BGK models (collision frequency employed as indicated) are shown together with the exact result (solid line) for comparison.

heat flux (see middle box at the bottom of Fig. 4). This is due to a much weaker decline of  $\nu_T \approx 1/y$  at large speeds and to a collisional deceleration being consequently more effective than obtained from the full collision operator.

Just as the temperature anisotropy, so does the heat flux decay much too rapidly if a constant collision rate  $\nu_{DT}$  or  $\nu_{FL}$  is employed in (6). This is illustrated in the last two boxes on the right-hand side. The very effective slowing down is caused by lack of the runaway effect for a constant  $\nu_c$  which therefore decelerates very fast particles as effectively as the thermal ones.

Figure 5 illustrates these results by another presentation. One-dimensional cuts through the distribution along the beam drift (magnetic field) direction are shown for six instances of time as indicated. The continuous curves display the collisional reshaping of the initially double-humped distribution towards a Maxwellian. As in earlier simulations<sup>5,6,35</sup> also in our present example, by employing the full collision term, thermodynamic equilibrium is achieved after about  $10\tau_0$ . In contrast, the BGK model with  $\nu_D$  (which is often used as a collision frequency in transport theory<sup>10,36</sup>) does not lead to a destruction of the beam. It remains resolved until the end of the numerical run. The collisional decay of the heat flux is somewhat more realistically described by  $\nu_F$ ; yet a slight skewness survives even after  $10\tau_0$ . As a result we can conclude that the BGK model is poor and insufficient as far as collisional evolution of moments higher than the pressure (or temperature) is concerned.

The numerical discrepancies as compared with the exact collision operator are striking, which is apparent from Table I(b). The maximum relative errors in the collisional invariants, the density, bulk speed, and temperature, are shown along with errors in the pressure ratio  $A = T_{||}/T_{\perp}$  and (final column) the normalized heat flux  $\hat{Q}_{||}$  obtained by numerically integrating the actual distribution:

$$\hat{Q}_{||} = \frac{\frac{1}{2} \int d^3v v_{||} (v_{||}^2 + v_{\perp}^2) f(\mathbf{v})}{\frac{3}{2} n v_0^3}. \quad (14)$$

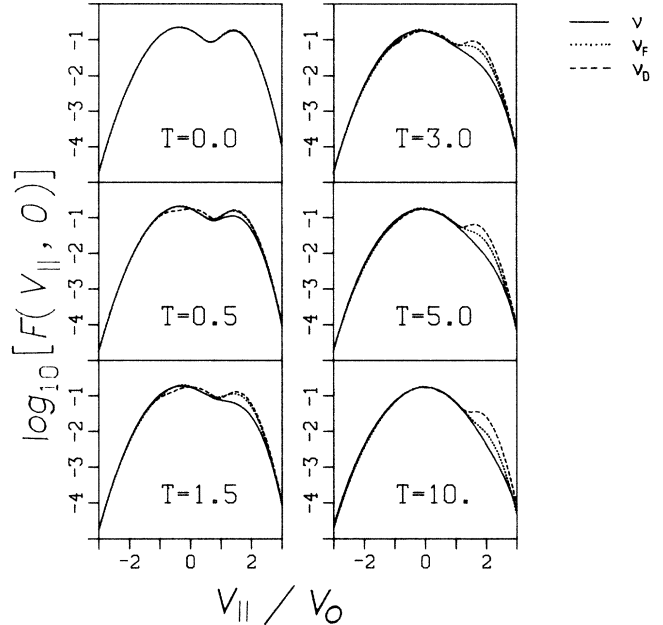


FIG. 5. Time sequence of one-dimensional cuts through the heat flux carrying distribution function as a function of parallel velocity component  $v_{||}$  in units of  $v_0$ . The exact result is shown by the solid line, whereas the BGK model results are shown by dotted ( $\nu_F$ ) and dashed lines ( $\nu_D$ ). Note the substantial differences in the time evolution of the beam according to the different collision operators used.

In addition, the average  $e$ -folding time  $\tau_c$  for the temperature isotropization is given. The exact result is  $\tau_c = (2.64 \pm 0.36)\tau_0$ ; see also Fig. 3. As for the bi-Maxwellian case, if the collision rate  $\nu_F$  is implemented in (6), we obtain smallest relative errors and best agreement. By comparison of the first three columns, one finds no substantial differences between results from the four rates as far as the conservation of density, speed, and temperature is concerned. This is understandable as by construction the BGK model for a constant collision rate should strictly conserve these quantities. However, for  $A$  numerical differences appear and even more substantial ones for  $Q$ , where intolerable errors occur. As a result, the BGK model has serious deficiencies in describing the collisional evolution of moments higher than the invariants  $n$ ,  $u$ , and  $T$ .

Model collision operators have been constructed to remedy this situation. Rawls *et al.*<sup>31</sup> established a Krook-type model with a self-adjoint operator, also satisfying the  $H$  theorem, with the rate function  $\nu_L$ . Basically, collisional relaxation is then forced toward a heat flux carrying distribution of the Grad type<sup>7</sup> which replaces the Maxwellian in the Krook model. However, the Rawls operator is an *ad hoc* approach and has not been derived from basic principles but mainly constructed such as to yield the same transport coefficients as derived from the full collision operator.

As our discussion has shown so far, the Krook model is unable to cope with the detailed shape of the distribution during the collisional evolution. This is again demon-

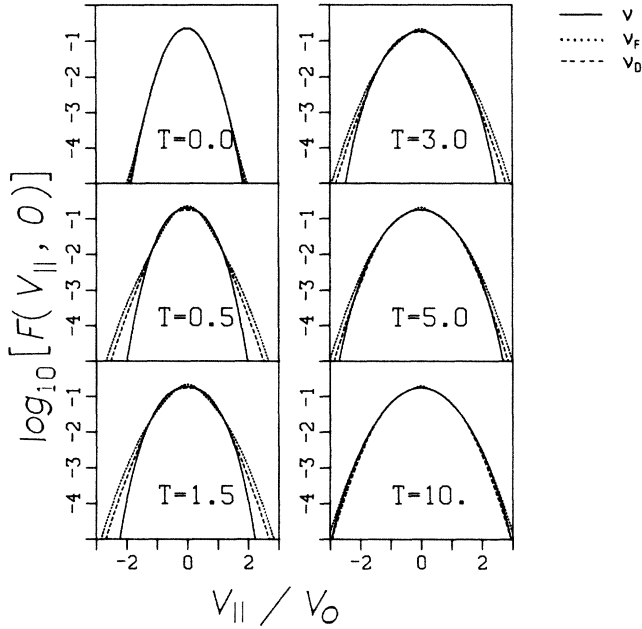


FIG. 6. Time sequence of one-dimensional cuts through the initially bi-Maxwellian distribution function as a function of normalized parallel speed. Solid line refers to the Fokker-Planck operator whereas dotted (dashed) lines display the BGK-model results with collision rate  $\nu_F$  ( $\nu_D$ ).

strated by Fig. 6, showing in the same format as Fig. 5, various one-dimensional cuts through the initial bi-Maxwellian distributions. Apparently, above the 1% level the curves for  $\nu_F$  and  $\nu_D$  and the exact result do not deviate much from each other. Below the 0.1% level in the tails substantial differences appear. For example, the exact collisional relaxation is slower there than implied by the Krook model. Only after  $10\tau_0$  is agreement between the various models found even in the far tails. The main reason for this behavior is that the effective rate  $\nu_{BGK}$  also depends on the ratio  $f_M/f$ , which is large at high speeds along the parallel axis, since initially  $T_{||} = 0.25T_{\perp}$ . Consequently,  $\nu_{BGK} \gg \nu$  and the Krook model unrealistically accelerates the relaxation process.

In order to illustrate the instantaneous relaxation rate associated with the actual shape of the distribution function we show in Figs. 7(a) and 7(b) one-dimensional spectra for two instances of time:  $t=0$  and  $t=3\tau_0$ . The distribution function along the beam direction is plotted versus the parallel speed for the exact rate  $\nu$  and the functions  $\nu_{F,L,D,T}$ . Upward arrows indicate instantaneous growth, downward pointing arrows mean negative rates yielding decay of phase-space density.

Apparently the implementation of the various rates in (6) leads to very different initial trends for reshaping the double-peak distribution [Fig. 7(a)]. The exact operator is associated with the largest negative collision rates at the beam position and only slight changes on top of the main

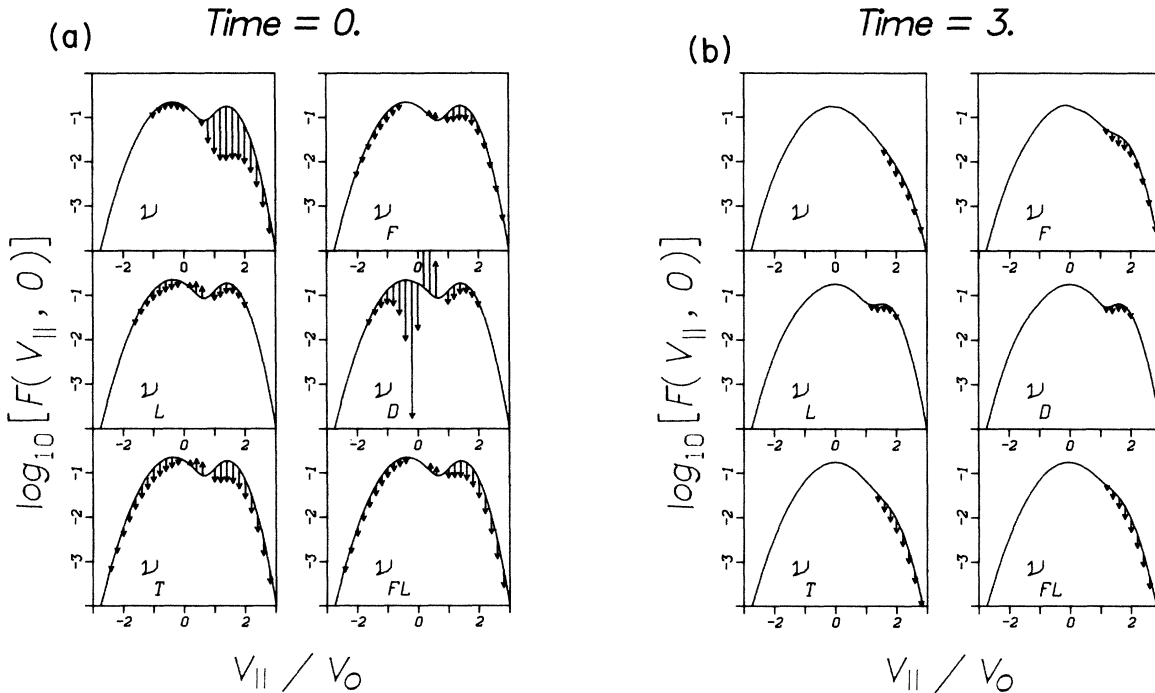


FIG. 7. One-dimensional cuts through the heat flux carrying distribution function at two instances of time (a) 0 and (b)  $3\tau_0$  plotted vs normalized parallel speed. The effective collision rate  $\nu$  and the various  $\nu_{BGK}$  are also shown by little arrows, the length of which gives the modulus of the rate. Upward pointing arrows mean positive and downward negative rates. Note the very different initial rates (a) and later on the differences in shape of the distribution at the original beam position.

peak. In contrast, all the other rates at the BGK model induce, to varying degrees, a reduction in phase-space density at both peaks, whereas between them positive rates are obtained leading to a filling up of the holes. A comparatively large effective collision rate for  $\nu_D$  results from the fact that  $\nu_D$  diverges at  $y=0$ . In contrast, the large negative rates for  $\nu$  at the beam are due to strong pitch-angle gradients in the beam regime (which are not taken into account by the BGK model) yielding enhanced collisional diffusion.

Figure 7(b) shows, in the same format as Fig. 7(a), the state of evolution at a later time  $t=3\tau_0$ . For  $\nu$  and  $\nu_T$  the peak is not resolved any more and only a heat-flux shoulder occurs. In contrast, for  $\nu_F$  and even more clearly for  $\nu_{L,D}$ , the second peak is still there and resembles its initial form.

These results are mainly due to the structure of the relaxation rates (see Fig. 1) at large speeds. The most rapid decline is obtained for  $\nu_D \approx 1/y^5$  favoring runaway for the beam particles (initial position  $y=1.4$ ). Although the actual  $f$  strongly deviates at the beam location from the equivalent Maxwellian, the longitudinal diffusion or deflection rate is too small to enforce "Maxwellianization" after  $3\tau_0$ . As a result, the collisional relaxation is drastically underestimated. Even after  $10\tau_0$  (not shown here) the peak survived as a nearly resolved plateau. This clearly illustrates the failure of the BGK model, if the Spitzer slowing down or deflection time is used for the collision rate  $\nu_c$ . It seems as if collisional runaway, as it occurs beyond the speed of the maximum of  $\nu_F$  in Fig. 1, can substantially be moderated by employing the full effective collision frequency.

#### IV. CONCLUSIONS

The collisional relaxation of a double-beam and a bi-Maxwellian distribution function has been studied by employing the BGK model<sup>1,15</sup> with various velocity-dependent relaxation times and by comparing its results with the exact ones obtained from numerical integration of the full Fokker-Planck collision integral.<sup>2</sup> This procedure allows us to assess the validity and reliability of the BGK operator not only qualitatively but, for the first time, quantitatively as well. Generally speaking, the Krook model may serve well to incorporate collisions in any model, as far as only their principal effects, for example on wave damping<sup>18,20</sup> are concerned. It has its merits in alleviating the tremendous problems arising in a fully consistent treatment of the Fokker-Planck or Boltzmann equation. However, our analysis shows that the results strongly depend on the choice of the relaxation rate employed, which has to be considered a free model function.

By construction, the BGK operator conserves density, momentum, and energy for a constant collision rate. If

the rate is velocity dispersive then this is no longer strictly true. Inspection of Table I shows that one can live with the induced numerical uncertainties. This near conservation of the collisional invariants of the Fokker-Planck or Boltzmann operator is the price to be paid for a better and somewhat more realistic treatment of the tails of the distribution function and of the higher moments as well. Still, the temperature anisotropy and the heat flux or skewness evolve quite differently in the true relaxation process as compared to any one of the discussed models, with the exception of the  $\nu_F$  model. The situation is much worse if a constant collision rate is employed for  $\nu_c$ . The evolution of  $A$  and  $Q$  is then entirely unrealistic. This result emphasizes the need to take the velocity dispersion of the collision rates  $\nu_c$  seriously into account.

Surprisingly enough, employing the rate  $\nu_F$  yields numerical results which come closest to reality and bear the smallest computational errors. As shown in Fig. 1,  $\nu_F$  starts linearly in  $y$ , then attains a maximum at about  $y=1$ , and asymptotically declines like  $1/y^2$  implying collisional runaway of the fast particles.<sup>37,38</sup> It seems as if these characteristics are essential for the fact that  $\nu_F$  reproduces most similarly the true collisional relaxation. Note that  $\nu_F$  naturally occurs in the frictional force term via the derivative of Rosenbluth's  $h$  potential<sup>2</sup> and that it substantially differs from Spitzer's slowing down rate  $\nu_L$  and deflection rate  $\nu_D$ , which are monotonically decreasing functions of the particle speed.

In conclusion, our analysis reveals that the BGK-model cannot be considered as generally appropriate for a description of the collisional relaxation of nonthermal distribution. If the friction rate  $\nu_F$  is employed this model reliably reproduces some qualitative features of the reshaping process of distributions, which initially deviate even strongly from Maxwellians. However, we would not recommend calculating transport coefficients with the BGK operator, since numerical errors must be expected to be intolerably large.

Still, it seems reasonable to start with the  $\nu_F$  relaxation-time model, if some principal effects of collisions are to be understood, i.e., in modifying the extreme effects of spatial inhomogeneity on velocity distributions of ions and electrons in dilute space plasmas. After our analysis we would not recommend, however, using such a model to investigate the spatial evolution of the heat flux carried by electrons in or beyond the runaway regime.<sup>39</sup> This warning particularly applies to the difficult situation where the heat flux carrying particles in the far tail represent a minority population (of a few percent or so), which is of the order of the relative density error unavoidably induced by using velocity-dispersive relaxation rates in the BGK model. In this case or whenever high numerical accuracy is required<sup>6,35,40</sup> the full Fokker-Planck equation must be solved.

<sup>1</sup>P. L. Bhatnagar, E. P. Gross, and M. Krook, Phys. Rev. **94**, 511 (1954).

<sup>2</sup>M. N. Rosenbluth, W. M. MacDonald, and D. L. Judd, Phys. Rev. **107**, 1 (1957).

<sup>3</sup>S. Chapman and T. G. Cowling, *The Mathematical Theory of*

*Non-uniform Gases*, 2nd ed. (Cambridge University, London, 1952).

<sup>4</sup>S. Chandrasekhar, Rev. Mod. Phys. **15**, 1 (1943).

<sup>5</sup>W. M. MacDonald, M. N. Rosenbluth, and W. Chuck, Phys. Rev. **107**, 350 (1957).

- <sup>6</sup>J. Killeen, A. A. Mirin, and M. E. Rensink, *Controlled Fusion*, Vol. 16 of *Methods in Computational Physics* (Academic, New York, 1976), p. 389.
- <sup>7</sup>H. Grad, *Commun. Pure Appl. Math.* **2**, 331 (1949).
- <sup>8</sup>S. I. Braginskii, in *Review of Plasma Physics*, edited by M. A. Leontovich (Consultants Bureau, New York, 1966), Vol. I, p. 205.
- <sup>9</sup>L. Spitzer and R. Härm, *Phys. Rev.* **89**, 977 (1953).
- <sup>10</sup>F. L. Hinton, in *Handbook of Plasma Physics, Basic Plasma Physics I*, edited by M. N. Rosenbluth and R. Z. Sagdeev (North Holland, Amsterdam, 1983), Vol. I, p. 147.
- <sup>11</sup>H. J. Fahr and B. Shizgal, *Rev. Geophys. Space Phys.* **21**, 75 (1983).
- <sup>12</sup>A. Hundhausen, *Solar Wind and Coronal Expansion* (Springer-Verlag, New York, 1972).
- <sup>13</sup>M. Schulz and L. J. Lanzerotti, *Particle Diffusion in Radiation Belts*, Vol. 7 of *Physics and Chemistry in Space* (Springer-Verlag, New York, 1974).
- <sup>14</sup>K. Jockers, *Astron. Astrophys.* **6**, 219 (1970).
- <sup>15</sup>E. P. Gross and M. Krook, *Phys. Rev.* **102**, 593 (1956).
- <sup>16</sup>R. L. Liboff, *Introduction to the Theory of Kinetic Equations* (Wiley, New York, 1969).
- <sup>17</sup>L. Spitzer, Jr., *Physics of Fully Ionized Gases*, 2nd ed. (Interscience, New York, 1962).
- <sup>18</sup>M. Porkolab, *Phys. Fluids* **11**, 834 (1968).
- <sup>19</sup>E. D. Heitowit and R. L. Liboff, *Phys. Fluids* **16**, 1446 (1973).
- <sup>20</sup>D. T. Farley, *J. Geophys. Res.* **68**, 6083 (1963).
- <sup>21</sup>T. F. Morse, *Phys. Fluids* **7**, 2012 (1964).
- <sup>22</sup>T. F. Morse, *Phys. Fluids* **6**, 1420 (1963).
- <sup>23</sup>J. D. Scudder and S. Olbert, in NASA Conference Publication No. 2280, 1983 (unpublished).
- <sup>24</sup>S. Olbert, in NASA Conference Publication No. 2280, 1983 (unpublished).
- <sup>25</sup>H. Rosenbauer, R. Schwenn, E. Marsch, B. Mayer, H. Miggenrieder, M. D. Montgomery, K.-H. Mühlhäuser, W. Pilipp, W. Voges, and S. M. Zink, *J. Geophys.* **42**, 561 (1977).
- <sup>26</sup>E. Marsch and S. Livi, *Phys. Fluids* **28**, 1379 (1985).
- <sup>27</sup>E. Marsch and S. Livi, *Ann. Geophys.* **3**, 545 (1985).
- <sup>28</sup>R. Hernandez and E. Marsch, *J. Plasma Phys.* (to be published).
- <sup>29</sup>R. Hernandez and E. Marsch, *J. Geophys. Res.* **90**, 11062 (1985).
- <sup>30</sup>B. S. Tanenbaum, *Plasma Physics* (McGraw-Hill, New York, 1967).
- <sup>31</sup>J. H. Rawls, M. S. Chu, and F. L. Hinton, *Phys. Fluids* **18**, 1160 (1975).
- <sup>32</sup>E. Marsch, K.-H. Mühlhäuser, R. Schwenn, H. Rosenbauer, W. Pilipp, and F. M. Neubauer, *J. Geophys. Res.* **87**, 52 (1982).
- <sup>33</sup>W. C. Feldman, J. R. Asbridge, S. J. Bame, and M. D. Montgomery, *Rev. Geophys. Space Phys.* **4**, 715 (1974).
- <sup>34</sup>S. Livi and E. Marsch (unpublished).
- <sup>35</sup>J. Killeen and K. D. Marx, in *Plasma Physics*, Vol. 9 of *Methods of Computational Physics* (Academic, New York, 1970).
- <sup>36</sup>T. J. M. Boyd and J. J. Sanderson, *Plasma Dynamics* (Nelson, London, 1969).
- <sup>37</sup>J. M. Burgers, *Flow Equations for Composite Gases* (Academic, New York, 1969).
- <sup>38</sup>H. Dreicer, *Phys. Rev.* **117**, 329 (1960).
- <sup>39</sup>J. D. Scudder and S. Olbert, *J. Geophys. Res.* **84**, 2755; **84**, 6603 (1979).
- <sup>40</sup>D. E. Fyfe and I. B. Bernstein, *Nucl. Fusion* **21**, 1581 (1981).